Global Ecology and Biogeography | A Journal of Macroecology | WILEY

Equilibrium in plant functional trait responses to warming is stronger under higher climate variability during the Holocene

Pierre Gaüzère[1] | Lars Lønsmann Iversen[1] | Alistair W. R. Seddon[2] | Cyrille Violle[3] | Benjamin Blonder[1]

[1]School of Life Sciences, Arizona State University, 427 E Tyler Mall, Tempe, Arizona 85281, USA

[2]Department of Biological Sciences and Bjerknes Center for Climate Research, University of Bergen, Bergen, Norway

[3]Centre d'Ecologie Fonctionnelle et Evolutive—UMR 5175 CEFE, Univ Montpellier, CNRS, IRD, EPHE, Univ Paul Valéry, Montpellier, France

Correspondence
Pierre Gaüzère, School of Life Sciences, Arizona State University, 427 E Tyler Mall, Tempe, AZ, 85281, USA.
Email: pierre.gauzere@gmail.com

Editor: Adam Tomasovych

Abstract

Aim: The functional trait composition of plant communities is thought to be determined largely by climate, but relationships between contemporary trait distributions and climate are often weak. Spatial mismatches between trait and climatic conditions are commonly thought to arise from disequilibrium responses to past environmental changes. We aimed to investigate whether current trait–climate disequilibrium is likely to emerge during plant functional responses to Holocene climate warming.

Location: North America.

Time period: 14–0 ka.

Major taxa studied: Terrestrial plants.

Methods: We joined global trait data with palaeoecological time series and climate simulations on 425 sites. We estimated plant community functional composition for three leaf traits involved in resource use. We then quantified disequilibrium in plant trait temporal responses to climate change during two contrasted periods: a period of high climate variability (14–7 ka) and a period of low climate variability (7–0 ka).

Results: Functional trait composition showed consistent deviation from climatic equilibrium during both periods. The temporal dynamics of trait composition tends to be positively correlated with climate equilibrium expectations during Holocene climate warming (14–7 ka), but not during a subsequent period of low climate variability (7–0 ka).

Main conclusions: Long-term functional responses of plants to climate change showed mixed evidence for both equilibrium and disequilibrium responses. Temporal trait dynamics were closer to the expectations of spatial dynamics under high climate variability, indicating that the relevance of space-for-time substitution might be dependent, in part, on climate variability. Our results also suggest that current mismatches between trait and climatic conditions might arise because of a divergence of factors influencing trait dynamics during periods of low climate variability. These findings provide a counterpoint to the common assumption that contemporary trait–climate mismatches result from lagged responses to past climate warming. Our study also demonstrates the need for a deeper investigation of the potential influence of non-climatic factors on functional plant community dynamics.

1 | INTRODUCTION

Variation in climate is often hypothesized to yield predictable variation in community functional composition (Enquist et al., 2015; Grime, 1974; von Humboldt et al., 1805; Webb, 1986; Woodward & Williams, 1987). The establishment of trait–environment relationships (TERs) is pivotal to our understanding and prediction of past, present and future biodiversity responses to climate change (Chave et al., 2009; Laughlin, 2014; Violle et al., 2014; Wright et al., 2004, 2005). These TERs can arise from environmental filtering because of variation in species performance along environmental gradients (Garnier et al., 2016; Keddy, 1992; Lavorel & Garnier, 2002). Trait responses to environmental variations are often assumed to be synchronous (the equilibrium hypothesis). However, contemporary spatial correlations between functional traits and climate have often been shown to be weak and inconsistent (e.g., Borgy, Violle, Choler, Garnier, et al., 2017; Bruelheide et al., 2018; Moles et al., 2014; Šímová et al., 2018). This has led to questioning of the robustness of many TER predictions across a range of organisms and spatial scales (Shipley et al., 2016).

Mismatches between climate and functional traits (functional disequilibrium) do not support the equilibrium hypothesis. They can be defined as the deviation between functional trait values observed in a given assemblage and the trait values expected from current climatic conditions. Functional disequilibrium is conceptually similar to the spatial mismatch observed between community composition and climatic conditions (climate disequilibrium or climatic debt; Bertrand et al., 2016; Davis, 1984; Svenning & Sandel, 2013), often defined as the deviation between climate niches observed in a given assemblage and the current climatic conditions. Mismatches between community and climate dynamics are likely to be common and widespread (Gaüzère, Iversen, Barnagaud, Svenning, & Blonder, 2018; Rohde, 2006), but we still have a limited understanding of their underlying processes (Blonder et al., 2017) and drivers (Bertrand et al., 2016).

A dominant hypothesis explaining contemporary functional disequilibrium lies in temporally lagged responses between trait and past climate dynamics (Blonder et al., 2018). According to this hypothesis, expressed here as the climatic mismatch hypothesis, climate determines the dynamics of trait composition, but functional disequilibrium results from a lagged response of trait composition to climate change (Blonder et al., 2017; Svenning & Sandel, 2013). The processes underlying climatic mismatches include taxon-specific processes, such as dispersal limitation, the persistence of long-lived species, speciation and adaptation (Davis, 1984; Enquist et al., 2015; Svenning & Sandel, 2013; Webb, 1986), in addition to community-scale temporal processes, such as memory effects (Blonder et al., 2017). However, the existence of disequilibrium between plant distribution and climatic conditions has been controversial. Some evidence supports the existence of disequilibrium dynamics, whereas other studies have found support for equilibrium between species distribution and climate at the millennial scale (Webb, 1986) and shorter (Williams et al., 2001). Climate mismatch patterns have also been interpreted as resulting from individualistic responses to different regional patterns of temperature and precipitation change (Webb, 1986; Williams & Jackson, 2007). The hypothesis of functional disequilibrium resulting from climatic mismatch is supported by empirical evidence of legacies from Late Quaternary climate change on contemporary trait distributions in Europe (Mathieu & Davies, 2014; Ordonez & Svenning, 2015, 2017; Svenning et al., 2015) and in the Americas (Blonder et al., 2018; Ordonez & Svenning, 2016).

A complementary hypothesis for the origin of functional disequilibrium lies in the impact of non-climate drivers (Pausas & Bond, 2019). According to the non-climatic hypothesis, non-climatic factors (i.e., biotic or abiotic factors not directly linked to climatic conditions) that vary over time could also select for certain species and influence trait composition (Sande et al., 2019). This hypothesis is supported by a growing body of evidence suggesting that plant assemblages can undergo rapid, widespread and long-lasting compositional change in response to human influence (Abrams & Nowacki, 2008; Bond et al., 2005; Keeley et al., 2011; Nowacki & Abrams, 2015), disturbance, land use and soil change (Borgy, Violle, Choler, Denelle, et al., 2017) or species interactions (Gill et al., 2009). These drivers are expected to be particularly important when they influence community dynamics against the backdrop of gradual climate change (Clifford & Booth, 2015).

These three hypotheses are not mutually exclusive and might have varying importance in time and space. However, many global change studies still operate under an assumption of equilibrium for forecasting contemporary the impacts of climate change based on contemporary spatial trait–environment relationships (S-TERs) (Violle et al., 2014). In other cases, temporal data have not been available to disentangle the processes underlying contemporary S-TERs. Consequently, most of the work investigating the origin of functional disequilibrium has relied on associations between contemporary spatial distributions of traits and snapshots of contemporary versus past climatic conditions (e.g., Blonder et al., 2018). The use of spatial patterns to infer temporal dynamics and processes (the space-for-time substitution approach) assumes that spatial and temporal biodiversity responses to environmental gradients are interchangeable (Pickett, 1989) and that changes in environmental conditions in time and space produce the same changes in functional composition of communities (Blois, Williams, Fitzpatrick, Jackson, et al., 2013). Given that most processes underlying the climatic mismatch hypothesis are temporal by nature, approaches relying on space-for-time substitution might provide limited inference on the

origins of contemporary mismatch between functional traits and climate distribution. To our knowledge, there has been no attempt to assess the influence of the three outlined hypotheses in a collective setting using long-term, large-scale temporal data.

Here, we developed an analysis framework to investigate the functional dynamics of North American plant communities using palaeoecological time series for 426 sites spanning the last 14 kyr in North America (Blois et al., 2011; Maguire et al., 2016). We coupled palaeoecological time series with functional trait information from global databases (Bjorkman, Myers-Smith, Elmendorf, Normand, Rüger et al., 2018; Kattge et al., 2020) and modern climate and palaeoclimate simulations over the study period (14–0 ka). To make concepts of "lag" and "mismatch" operational and measurable, we developed an analysis based on a framework using community response diagrams (Blonder et al., 2017; Gaüzère et al., 2018). The approach compares the site-scale temporal response of community functional composition to climate changes, or temporal trait–environment relationships (T-TERs) with global-scale spatial patterns of trait–environment associations (S-TERs) (Figure 1). This approach provides a tool to test the temporal processes influencing

trait–environment disequilibrium through time, where S-TERs are used as a reference describing which community trait values can be expected given local climatic conditions. We estimated S-TERs from an independent, global and contemporary dataset as a reference of trait values expected in climatic conditions (see Supporting Information Figure S1; Text S1). Although S-TERs estimated from contemporary data are probably not exempt from disequilibrium, they represent the best global TER estimation currently available (Bruelheide et al., 2018). Temporal dynamics of palaeo-assemblage trait values and reconstructed maximum temperature were used to assess, for each palaeosite, the T-TER during the Holocene.

We compute three statistics quantifying the match between T-TERs and S-TERs and the complexity of temporal dynamics: the response fit $\geq \rho$, which quantifies the correlation between T-TER and S-TER; the absolute deviation (Λ), which indicates the average difference between T-TER and S-TER; and the state number (n), which indicates the maximum number of possible community mean trait values observed for a given temperature value (Figure 1). Each statistic quantifies a particular aspect of disequilibrium dynamics, such as lag, nonlinearity or multiple stable states. They can be used to

FIGURE 1 Trait–environment relationships (TERs) via community response diagrams (CRDs). For each site, the community mean trait value (*y* axis) and maximum annual temperature (*x* axis) are combined in a time series plot to estimate site-specific temporal trait–environment relationships (T-TERs). The time series dynamics are contrasted to the mean spatial trait–environment relationship (S-TER). The CRD framework is used to estimate three summary statistics for each site: the correlation between S-TER and T-TER (response fit, ρ), the spatial–temporal disequilibrium (absolute deviation, Λ) and the presence of alternative states in the T-TER (state number, *n*). Site a exemplifies summary statistics when S-TER and T-TER are matching; site b illustrates mismatch whereby S-TER and T-TER are inversely correlated but without any alternative state; and site c illustrates another mismatch example whereby S-TER and T-TER are not correlated and the temporal response exhibits alternative states
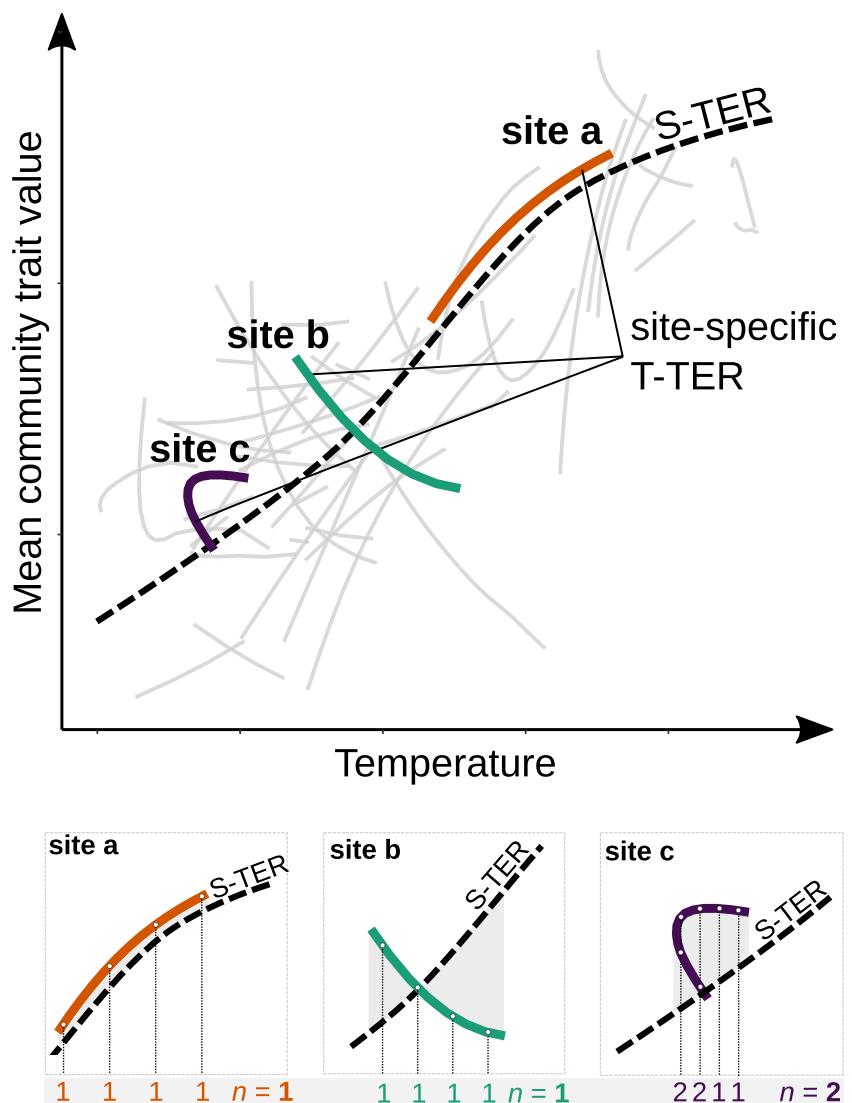
characterize a continuum of simple-to-complex response scenarios of traits to climate change (Blonder et al., 2017; Gaüzère et al., 2018). We focused on three functional traits related to plant ecological strategies and resource use (Pierce et al., 2017; Wright et al., 2004) and expected to be constrained by climatic conditions (Borgy, Violle,

Choler, Denelle, et al., 2017; Wright et al., 2005, 2017): leaf area, specific leaf area (SLA) and leaf dry matter content (LDMC). We used maximum annual monthly temperature as a main climate descriptor because it is a reliable and integrative variable to predict responses to climate change during the study period (Blois, Williams, Fitzpatrick,
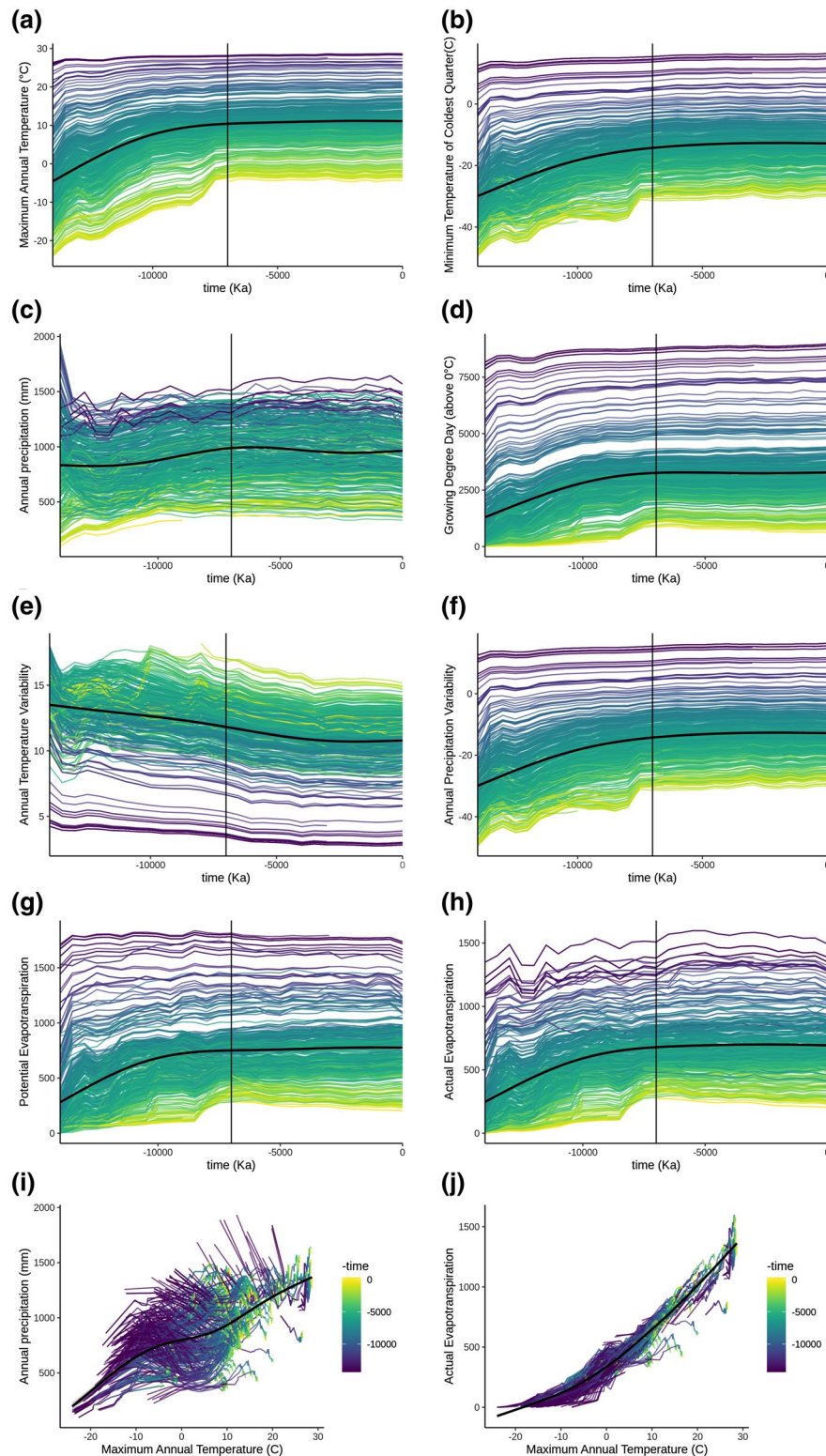
FIGURE 2 Climate change during high- and low-variability periods. (a–h) Temporal dynamics of climate variables during the study period. Each coloured line is the time series of a given site, and colour indicates the latitude. The black shaded curve represents the overall nonlinear dynamic (estimated from Generalized Additive Model) over the two periods. These different temperature dynamics were used to segregate two different periods, 14–7 ("high variability") and 7–0 kyr BP ("low variability"), with the vertical black line showing the separation between the two periods. (a) Maximum annual temperature. (b) Minimum temperature of the coldest quarter. (c) Annual precipitation. (d) Growing degree days > 0 °C. (e) Annual temperature variability. (f) Annual precipitation variability. (g) Potential evapotranspiration. (h) Actual evapotranspiration. (i, j) Spatio-temporal correlation plots between mean annual temperature and mean annual precipitation (i) or actual evapotranspiration (j). Plots are qualitatively similar for growing degree days > 0 °C and potential evapotranspiration

Ferrier, et al., 2013; Lorenz, Nieto-Lugilde, Blois, Fitzpatrick, & Williams, 2016; Maguire et al., 2016). Temperature was also the most dynamic climatic variable during the study period, and it was closely correlated in space and time with many bioclimatic variables known to drive plant community composition (Figure 2). Temperature variations during the study period exhibited two contrasted regimes, allowing us to make predictions for all hypotheses across space and time: a first period marked by high climate variability with increasing temperature between 14 and 7 ka, and a second period of low climate variability and slow temperature changes between 7 and 0 ka (Figure 2). We repeated our analyses based on annual precipitation as a climate descriptor (see Supporting Information Figure S2; Tables S1 and S2).

Although the estimation of T-TERs during the Holocene carries a significant amount of uncertainty linked to the spatial and temporal resolution of palaeoecological data (Brewer et al., 2012), this framework allowed us to explore evidence for the following hypotheses. According to the equilibrium hypothesis, contemporary functional disequilibrium is independent from past environmental conditions. We expect a strong match between temporal responses and spatial associations during periods of both high and low climate variability. This functional response corresponds to a "no-lag" response scenario (Blonder et al., 2017; Gaüzère et al., 2018) and is ideally identified by a positive correlation between T-TER and S-TER ($\rho \approx 1$), a low deviation from expected values ($\Lambda \approx 0$), and one community mean trait value for each climate value ($n = 1$). According to the climatic mismatch hypothesis, we expect a trait–climate match during low climate variability because functional composition can change fast enough to adjust to climatic variations. During low climate variability, we predict a positive correlation between T-TER and S-TER ($\rho \approx 1$), a low deviation from expected values ($\Lambda \approx 0$), and one community mean trait value for each climate value ($n = 1$). Conversely, we expect mismatch responses during a period of high climate variability, with response scenarios such as a lagged response, memory effects and alternative states identified by the absence of a positive correlation between T-TER and S-TER ($\rho \neq 1$), a strong deviation from expected values ($\Lambda > 0$), and more than one community mean trait value for each climate value ($n > 1$). According to the non-climatic hypothesis, we expect mismatches between functional and climate dynamics to occur during low climate variability rather than during climate warming (Clifford & Booth, 2015). This hypothesis extends the "equilibrium hypothesis", while considering the effect of non-climatic factors; that is, climate remains the stronger driver of temporal dynamics during high climate variability. However, climatic selection pressure is overridden by non-climatic factors during low climate variability and generates apparent trait–climate mismatch (Clifford & Booth, 2015). In this case, we expect a strong match between temporal responses and spatial associations during high climate variability, identified by a positive correlation between T-TER and S-TER ($\rho \approx 1$), a low deviation from expected values ($\Lambda \approx 0$), and one community mean trait value for each climate value ($n = 1$). During the period of low climate variability, we expect more complex scenarios characterized by the lack of positive correlation between T-TER and

S-TER ($\rho \neq 1$), deviation from expected values ($\Lambda > 0$), and more than one community mean trait value for each climate value ($n > 1$).

When applied to long-term ecological data, these predictions enable us to examine the continuum of long-term, functional community responses to climate change and to determine which hypotheses of functional disequilibrium origins are the most likely to underlie observed dynamics. Owing to the scarcity of trait measurements, in addition to the limited quality and resolution of palaeoclimate and non-climate data over long time periods and large spatial scales, it is not possible to falsify all hypotheses rigorously in all cases (Platt, 1964). Nevertheless, our approach is able to provide partial insight into support for each hypothesis. The equilibrium hypothesis can be rejected preliminarily if any evidence is found for disequilibrium over time (allowing for the possibility that unmeasured or inaccurate data can limit inference); the climate mismatch hypothesis can be rejected preliminarily if the available climate data do not yield lagged dynamics (also allowing for data quality issues); and the non-climate hypothesis can be supported preliminarily if (by a process of elimination) both of the other hypotheses are rejected (because no direct tests are yet possible, owing to the lack of high-resolution data for potential non-climate impacts; see Discussion).

2 | METHODS

2.1 | Data

2.1.1 | Community composition

We did not process the pollen data, but obtained plant community compositions directly from the fossil pollen dataset used by Maguire et al. (2016). This dataset is a selection of sites and revised, standardized chronologies updated to the IntCal09 calibration curve from Blois, Williams, Fitzpatrick, Ferrier, et al. (2013), which was extracted from the Neotoma Paleoecology Database (Williams et al., 2018; www.neotomadb.org) and contributions from individual researchers. We refer to this dataset as the "Neotoma dataset". This selection provides high-quality time series assemblages on 531 sites primarily located in eastern North America. Pollen abundances are expressed as the pollen sum for a particular taxon divided by the total sum for all genus-level taxa. Pollen relative abundances were interpolated to 500-year time slices from 21 ka to the present; for each time period, only sites with a weighted quality value > .75 were included. The relative abundance pollen matrix was converted to a presence/absence matrix after applying a threshold scaled to 5% of the maximum abundance (Nieto-Lugilde et al., 2015). Given that the majority of fossil pollen types considered here can be identified consistently, absences are considered true absences. We chose the 19 most abundant-through-time taxa at the generic level.

Pollen assemblages obtained from lake sediments provide a rough proxy for the composition of communities, despite issues on spatial and taxonomical scale integration, species abundance versus pollen abundance, and the detectability of rare taxa (Birks

& Seppä, 2004). These issues might influence the quantification of functional composition because taxonomic definition is mostly limited to genus, and rarer taxa with lower dispersal abilities might be undetected. We limited our analysis to a subset of data including time series > 5,000 years over the whole study period. The overall process yielded a genus-level presence/absence dataset comprising 425 sites, 103 plant taxa and 45 time bins (500 years each) spanning 21 ka to the present. The resulting dataset is the same as the one used by Gaüzère et al. (2018). More details on pollen data quality and site selection are provided by Blois, Williams, Fitzpatrick, Ferrier, et al. (2013). Further modifications, site and taxa selection, and time interpolation are provided by Maguire et al. (2016).

2.1.2 | Traits

We focused our study on three leaf traits involved in resource acquisition and use: leaf area, leaf area per leaf dry mass (specific leaf area, SLA) and leaf dry mass per leaf fresh mass (leaf dry matter content, LDMC). This set of traits is particularly suitable for testing hypotheses related to plant–climate relationships because they are thought to be linked to major axes of plant ecological strategy (Westoby et al., 2002; Wright et al., 2004). We compiled a set of > 420,000 contemporary observations of trait values from the TRY (Kattge et al., 2011) and TTT (Tundra Trait Team database; Bjorkman, Myers-Smith, Elmendorf, Normand, Thomas et al., 2018). We chose to mix these two datasets in order to sample values of traits across the large range of climate conditions experienced by plants during the study period in North America. We used the observations from TRY and TTT to compute species- and genus-level average trait values of taxa present in the palaeocommunities. We removed duplicate occurrences, checked units and removed observations with homonyms and obvious location errors. We then computed, for each trait and each genus, the mean and the standard deviation of $\log_{10}$-transformed trait values.

Given that palaeoecology databases relying on fossil pollen are still limited in terms of taxonomic resolution, we paid a particular attention to the choice of functional traits displaying strong correlation and low dispersion between species- and genus-scale mean trait values. We checked for the taxonomic conservatism of averaged trait values between the genus and species scale. We computed separately the leaf area, SLA and LDMC species- and genus-scale mean trait values and investigated the correlation and the dispersion between species and genus mean trait values. Leaf area, SLA and LDMC showed strong correlation and low dispersion between species- and genus-scale mean trait values. These results provide support for the use of genus-scale average trait values. All details on data, processing, the number of observations per trait, estimations and comparison of species- and genus-scale mean trait values and climate coverage are provided in the Supporting Information (Text S1).

2.1.3 | Climate

We based our analyses on the maximum annual monthly temperature as a unique climate descriptor, for several reasons. First, it is a good predictor of species and community responses to climate change since the Last Glacial Maximum (Blois, Williams, Fitzpatrick, Ferrier, et al., 2013; Maguire et al., 2016). In particular, a study based on the same dataset (Blois, Williams, Fitzpatrick, Ferrier, et al., 2013) showed that summer temperature was the only consistently important predictor of community composition change during the study period, whereas mean precipitation, mean temperature for winter (December–February), temperature seasonality and precipitation seasonality did not show any consistent effect. Second, it is the climatic variable for which palaeoclimate models are the most accurate, with fewer uncertainties (Lorenz et al., 2016). Third, it is an integrative climate axis whose temporal dynamics are highly correlated in space and time with many bioclimatic variables (Figure 2). Fourth, the temperature dynamics during the last 14 ka clearly exhibit two distinct periods of high and low variability within the study area, further supported by the dynamic of other bioclimatic variables (growing degree day, actual evapotranspiration, potential evapotranspiration, temperature seasonality and precipitation seasonality; Figure 2). Note that we also ran our analyses based on the annual precipitation in order to check the consistency of results between that maximum annual monthly temperature and annual precipitation (Supporting Information Figure S2; Tables S1 and S2).

Contemporary climate data (1979–2013 AD averages) for maximum annual temperature based on monthly temperature (MAT) and mean annual precipitation (MAP) were obtained from the CHELSA dataset v.1.2 (available at: https://chelsa-climate.org/; Karger et al., 2017). CHELSA (Climatologies at High resolution for the Earth's Land Surface Areas) is a high-resolution (30 arc s) climate dataset for the Earth's land surface areas based on a quasi-mechanistic statistical downscaling of the ERA (European Re-Analysis) interim global circulation model with a GPCC (Global Precipitation Climatology Centre) bias correction, and incorporating topoclimate (Karger et al., 2017). Derived parameters are estimated on a monthly basis and independent of biases inherent to interpolation between weather stations with uneven coverage of geographical and climate space.

Palaeoclimate data (from 22 ka to the present) for maximum annual temperature based on monthly temperature and bioclimatic variables [Figure 2; mean annual precipitation, growing degree days (> 0 °C), actual evapotranspiration, potential evapotranspiration, temperature seasonality and precipitation seasonality] were obtained from SynTraCE-21, a set of transient simulations run using the CCSM3 model (Liu et al., 2009). The model includes transient forcing changes in greenhouse gases, orbitally driven insolation variations, ice sheets and meltwater fluxes. These simulations are reasonably congruent with site-based climate reconstructions (Harrison et al., 2014). Simulations were statistically downscaled to a 0.5° × 0.5° grid cell, and then, for every 500 years from 14 to 0 kyr BP, average climate variables were calculated based on a 200-year window centred

on the 500-year time step (Lorenz et al., 2016). The dynamics of several climate variables [MAT, MAP, growing degree days (> 0 °C), actual evapotranspiration and potential evapotranspiration] extracted from (Lorenz et al., 2016) are shown in Figure 2.

2.2 | Analysis

2.2.1 | Spatial trait–environment relationships

We inferred spatial trait–climate relationships based on observations of functional traits from the TRY and TTT databases. We selected all trait measurements with spatial coordinates and extracted the corresponding contemporary MAT from the CHELSA climate model. For each trait, we modelled the nonlinear relationship between individual functional trait values (response variable) and the maximum annual temperature (explanatory variable) fitted using smoothing splines with a free degree of freedom. To account for variability between sites and origins of data, the site was considered as a random effect (intercept) in the models. These additive relationships provide an independent assessment of spatial trait–climate relationships that can be compared with temporal dynamics within each site. Spatial trait–environment relationships estimated for leaf area, SLA and LDMC displayed contrasting patterns (see Figure 2). Leaf area showed a steady increase with increasing maximum annual temperature. Apart from local nonlinear variation, SLA showed a bell-shaped relationship with temperature, peaking at 12 °C. LDMC was not consistently related to maximum annual temperature. These contrasting spatial patterns were then used to infer an association between S-TERs and T-TERs. Note that linear and quadratic S-TERs for both maximum temperature and precipitation were also estimated, from both contemporary trait data (TRY–TTT) and palaeocommunity composition (Neotoma). All S-TERS are displayed and compared in the Supporting Information (Figure S1). Supplementary analysis revealed consistent qualitative patterns between TERs estimated from palaeo or contemporary data. Note also that results produced using contemporary climate data and palaeo-trait and palaeoclimate data were qualitatively similar (Supporting Information Figure S3; Table S3).

2.2.2 | Temporal trait–environment relationships

For each site/trait time series, we estimated the temporal relationship between community mean trait value and MAT (T-TER). We computed community functional trait means using community composition from Neotoma and genus-scale average trait values previously calculated from TRY and TTT observations (see section 2.1.2 | Traits). We extracted maximum annual temperature data from the CCSM3 model for each site/date paired to the Neotoma dataset (Lorenz et al., 2016). We then smoothed community functional trait means and mean annual temperature times series using locally estimated scatterplot smoothing (LOESS). LOESS was performed for each time series independently using the loess {stats} R

function with an α span of 0.75. Smoothing the time series has the advantage of reducing: (a) the inter-annual variability and temporal stochasticity that might undermine the identification of community and climate dynamics; and (b) the difference in uncertainty between periods that might ultimately influence observed differences in statistics (Tomasových & Kidwell, 2010). Owing to the greater environmental and trait changes that occurred (by definition) during the period of high climate variability, this period was associated with higher T-TER-explained variation (high-variability period mean $\pm$ SD $r^2 = 0.79 \pm 0.322$, low-variability climate period mean $\pm$ SD $r^2 = 0.42 \pm 0.342$). For each site and each period, T-TER was built by sequentially plotting the smoothed community functional trait mean time series over the smoothed MAT time series (Figure 1).
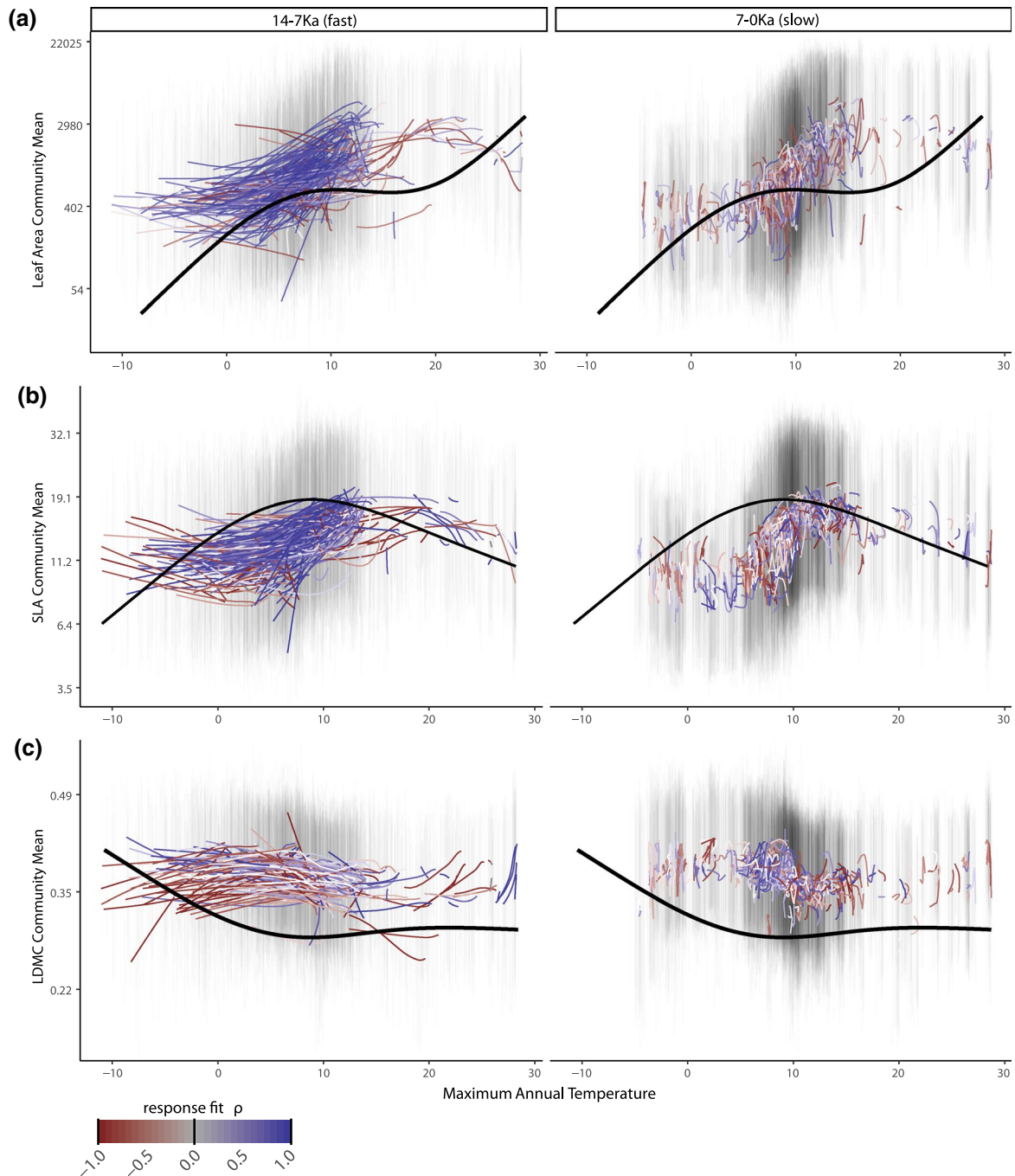
2.2.3 | Community response diagrams

We used the community response diagram (CRD) framework (Blonder et al., 2017; Gaüzère et al., 2018) to quantify disequilibrium between spatial and temporal trait–climate relationships. Previous applications of this framework were based on the response of community inferred temperatures to changes in observed temperatures, assuming equilibrium dynamics (i.e., equality, between these two variables). Here, we extended the approach to account for the nonlinear nature of trait–environment relationships expected at equilibrium by comparing the equality of predicted values of an S-TER versus T-TER (see Figure 1). We quantified the match between spatial and temporal patterns using three descriptive statistics derived from response diagrams (Figure 1).

The response fit, ρ, quantifies the correlation between the temporal and spatial community trait response to mean annual temperature. It is calculated as the Spearman's correlation coefficient between temporal and spatial trait means paired by temperature values. Given that the distribution of ρ was not normal, we used the nonparametric, one-sample Wilcoxon signed rank test to detect significant deviation from zero (i.e., null hypothesis, H_0: median ρ = 0).

The absolute deviation, Λ, quantifies the average, time-invariant disequilibrium between the S-TERs and T-TERs. For each site, it is calculated as the mean absolute deviation between temporal and spatial trait means paired by temperature values. We used Student's one-sample t-tests to detect a significant positive deviation from zero (i.e., null hypothesis H_0: mean $\Lambda = 0$ and H_1: mean $\Lambda > 0$).

The state number, n, quantifies the maximum number of (smoothed) mean trait values (y axis in CRD) that correspond to a given single value of observed maximum temperature (x axis in CRD). It is calculated as the maximum number of times a vertical line in each of the time series on the diagram crosses a given T-TER. Temporal stochasticity and sampling error tend to inflate the state number through the detection of more than one community state which is statistically not different. To correct for this false detection of $n > 1$, we tested for the difference between community mean trait values by comparing the difference between the 95% confidence interval associated with each community mean trait value. If the 95%

FIGURE 3 Spatial and temporal trait–environment (S-TER and T-TER) relationships in North American plant communities. Stacked community response diagrams for each trait and period. Coloured lines correspond to site-specific T-TERs during the 14–7 ka "high climate variability" (left) or 7–0 ka "low climate variability" (right) period, with line colour indicating the value of response fit, ρ (i.e., the Spearman correlation coefficient between T-TERs and S-TERs, from red = −1 to white = 0 to blue = 1). The black shaded curve represents the reference S-TER. Grey vertical lines show the propagated error associated with raw community trait means (mean ± *SEM* of the trait individual trait distribution)

confidence intervals were overlapping, we inferred that the community mean trait values could not be differentiated and reduced *n* by one. More details, formalization and simulations of CRDs are provided by Blonder et al. (2017) and Gaüzère et al. (2018).

Statistics were computed for each site over each period separately. Both periods shared a similar number of sites (304 sites for 14–7 ka and 358 sites for 7–0 ka). Time series were generally longer

for the 7–0 ka period (average 6,851 years) than for the 14–7 ka period (average 4,456 years). To ensure that the difference in the length of time between the two periods could not drive the difference observed in summary statistics, we randomly sampled eight data points (i.e., 4,000 years) in each site/period time series. Time series < 4,000 years were removed from this ancillary analysis. Subsampling a constant number of data points between each period

GAÜZÈRE ET AL.

Global Ecology
and Biogeography

A Journal of
Macroecology

WILEY 9

did not affect our results qualitatively. More details on the analysis and results are provided in the Supporting Information (Figure S4).

3 | RESULTS

During the period of high climate variability (14–7 ka), T-TERs were positively correlated with expectations from S-TERs for most of the sites (Figure 3), as shown by the distribution of response fit (Figure 4). During the period of low climate variability (7–0 ka), T-TERs were uncorrelated with expectations from S-TERs for most of the sites

(Figures 3 and 4). The response fit, ρ, measured for each site as the correlation between T-TER and S-TER, showed contrasting patterns between traits and periods. During the period of high climate variability (14–7 ka), distributions of ρ were significantly skewed towards one for leaf area and SLA (Figure 4a,b). For LDMC, ρ values appeared uniformly distributed, without significant deviation from zero (Figure 4c). During the stable period (7–0 ka), ρ values were uniformly distributed for all traits, without significant deviation from zero for leaf area (Figure 4a), SLA (Figure 4b) or LDMC (Figure 4c). Statistical details of underlying nonparametric tests are presented in the Supporting Information (Table S5).
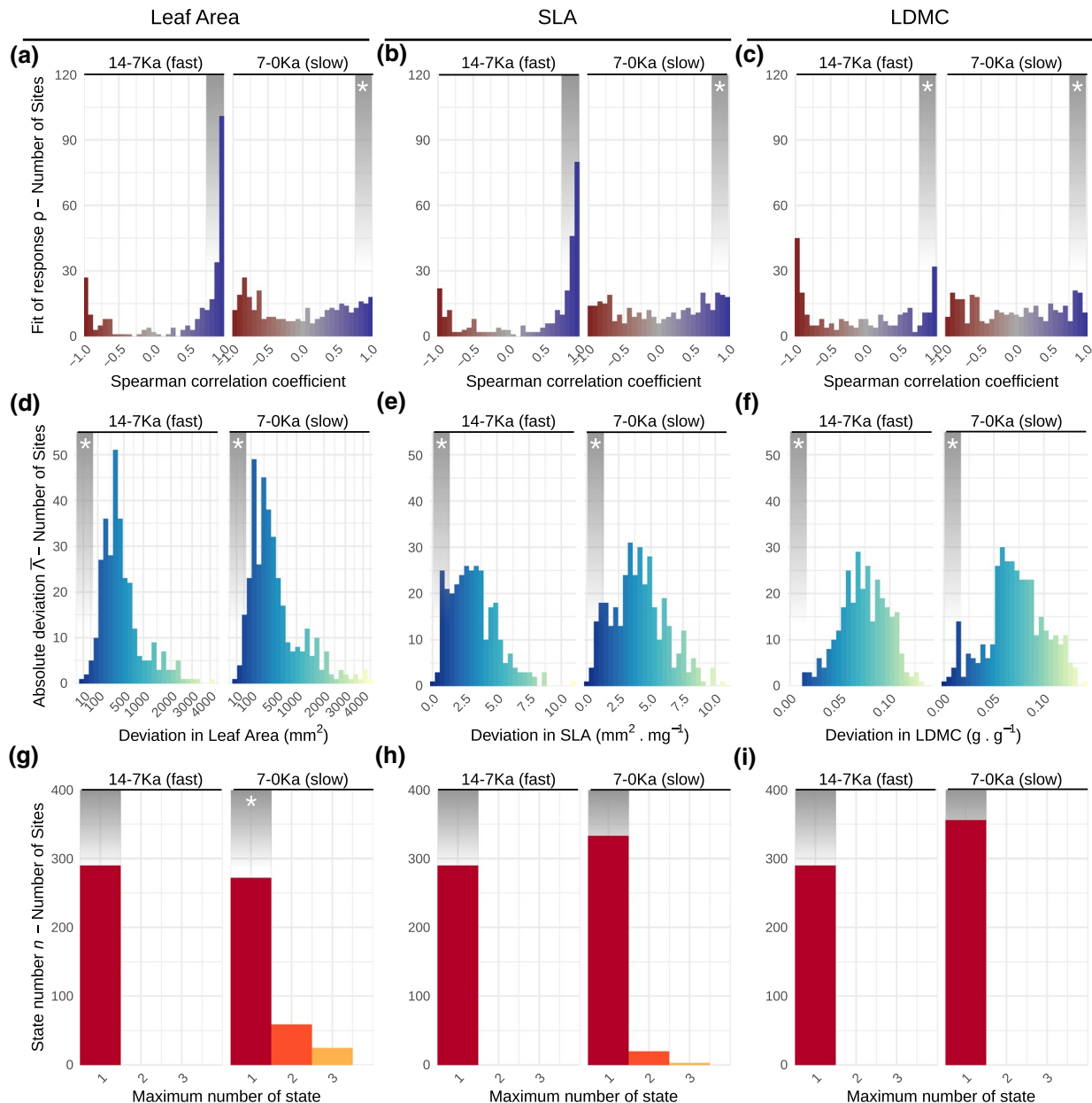
FIGURE 4 Distributions of summary statistics (rows) for each functional trait (columns). (a,d,g) Response fit (ρ). (b,e,h) Absolute deviation (Λ) expressed in natural units of traits (see y axis title). (c,f,i) State number (n). Note that labels indicating Λ values were back-transformed to original units; therefore, the x axis scales are not linear. Shaded area in the top of each histogram represents expectations under the equilibrium hypothesis ($\rho \approx 1$, $\Lambda \approx 0$, $n = 1$). A white asterisk within the shaded area indicates that the distribution diverges significantly from this hypothesis

The absolute deviation, Λ, was consistently large and revealed significant differences between T-TERs and reference contemporary S-TERs across traits and periods. During the warming period, the average absolute deviation of leaf area was 562 (495, 628) mm^2 (lower and upper 95% confidence interval; Figure 4d), for SLA 3.2 (2.9, 3.4) mm^2/mg (Figure 4e) and for LDMC 0.074 (0.072, 0.077) g/g (Figure 4f). During the stable period, the average absolute deviation of leaf area was 614 (534, 693) mm^2 (Figure 4d), for SLA 4.1 (3.8, 4.3) mm^2/mg (Figure 4e) and for LDMC 0.072 (0.069, 0.075) g/g (Figure 4f). Statistical details of underlying parametric tests are presented in the Supporting Information (Table S5).

The state number, n, was generally low, suggesting that assemblages rarely display alternative functional states. A value of $n = 1$ was observed during the period of high climate variability for all sites and all traits, indicating that the functional composition of communities displayed only a single value for a given temperature. During low climate variability, n ranged from one to three, depending on sites and traits. Only leaf area showed significant departure from $n = 1$, with 24% of the sites having more than one realized state for a given observed temperature (Figure 4g). For SLA, 7% of the sites exhibited multiple values for a single observed temperature (Figure 4h). For LDMC, only two sites (of 358 sites present in this period) had $n > 1$ (Figure 4i). Statistical details of underlying parametric tests are presented in the Supporting Information (Table S6).

These results, based on the functional response to annual mean temperature, were consistent with analyses based on precipitation (Supporting Information Figure S2; Tables S1 and S2) and more complex bioclimatic features (given the close correlation in space and time; Figure 2). Analyses based on S-TERs estimated from palaeoecological rather than contemporary data (Supporting Information Figure S1) showed similar qualitative results. In particular, the response fit, ρ, was significantly skewed towards one during the period of high climate variability, randomly distributed during the period of low climate variability for all traits, and the absolute deviation, Λ, was generally lower (Supporting Information Figure S3).

4 | DISCUSSION

Our study provides a temporally and spatially resolved assessment of how functional composition responds to climate variation. Our results provide a partial assessment of multiple hypotheses for drivers of the observed functional dynamics. First, our results bring mixed support for the equilibrium hypothesis. In line with Blois, Williams, Fitzpatrick, Jackson, et al. (2013), we found a tendency for a rapid and adjusted functional response during high climate variability. However, adjusted responses were not observed during the period of low climate variability, and substantial deviations were observed during both periods. This suggests that equilibrium responses might not be always present and challenges the assumption of equivalence between spatial and temporal responses under weak climate forcing. Second, our results seem to reject the climate mismatch response hypothesis. We observed a tendency towards matching trait–climate

responses during the period of high climate variability, suggesting that functional community composition can track climate over millennia time-scales when temperature increases [i.e., 1.6 ± 0.62 °C/kyr (mean ± SD)]. Third, we showed a tendency towards trait–climate decoupling during the period of low climate variability rather than during the period of high variability. Our data prevent us from determining the particular drivers of the community response during stable climate. However, within the resolution and accuracy of available palaeoclimate data, we can determine that changes in neither mean annual temperature nor annual precipitation are sufficient explanations for the trait–climate decoupling observed during the late Holocene. We observed a consistent absolute deviation from climate equilibrium during both periods. Although this result does not clearly follow any of our hypotheses, several potential interpretations can be drawn. First, absolute deviation might arise from trait–climate disequilibrium in the contemporary S-TERs, because current trait distribution is affected by a lagged response to recent climate change and/or human influence. Second, particular taxa in the pollen data might be underrepresented when compared with contemporary data. This might be the case particularly for alpine and arctic tundra shrubs. Absolute deviation might arise from this discrepancy in the representativity of taxa. These two potential explanations are supported by the fact that the absolute deviation values estimated with palaeo S-TERs as a reference were lower (Supporting Information Figure S3). Finally, a last explanation lies in the imprint of non-climatic drivers affecting trait composition on top of the climate signal for both periods.

Overall, our findings do not support the hypothesis that contemporary functional disequilibrium results from lagged responses to past climate warming (Blonder et al., 2018; Ordonez & Svenning, 2015, 2017). This is in line with the idea that taxon-specific climatic responses during the Holocene match changes in temperature (Webb, 1986). Our data indicate support for asynchronous, complex response scenarios triggering temporal decoupling between functional composition and climate change during low climate variability. This line of evidence suggests that against the backdrop of weak climatic variation, non-climatic factors might affect functional plant community composition and generate discrepancies in trait–environment relationships.

Our results confirm that community temporal response to climate change does not always follow simple or consistent rules across time and space (Gaüzère et al., 2018) and suggest that the intensity of the climate forcing might be an important determinant of such responses. This might be particularly relevant for forecasting the climate response, because temperature increases during the period of high climate variability 14–7 ka are roughly comparable to contemporary climate change in some localities (Willis & MacDonald, 2011). The space-for-time substitution inherent to many anticipatory predictions from species distribution models appears dependent on the intensity of climate variation, which calls for caution when forecasting functional community responses to contemporary global change. The constant-lag (or no-lag, when considering palaeo S-TERS; Supporting Information Figure S3) functional response observed

during the period of high climate variability contrasts with the complex temporal dynamics (e.g., stochastic responses, lags and alternative states) reported from the species composition of the same pollen assemblages during the same period (Gaüzère et al., 2018). It is, however, consistent with the idea that many functional traits are constrained by climatic conditions in space and time (Muscarella & Uriarte, 2016), whereas the temporal response of species compositions are less predictable and more subject to species-specific responses (Bertrand et al., 2016; Blois, Williams, Fitzpatrick, Jackson, et al., 2013; Svenning et al., 2015). Based on the available climate data, we also showed low "response fit" of plant communities during low climate variability. According to the climatic mismatch response hypothesis, one would expect a stronger match between spatial and temporal functional trait responses across shorter climatic gradients. We observed a tendency towards a more positive response fit during the warming period, which exhibited an average temperature increase 16 times stronger than the period of low temperature variability. Consequently, we found little support for the climatic mismatch response hypothesis within North American plant communities. These results contrast with the idea that current functional disequilibrium accumulated during Late Quaternary climate change (Ordonez & Svenning, 2015, 2017) because of lagged assemblage responses to temperature and precipitation changes (Blonder et al., 2018).

Our study suggests that current functional disequilibrium might have accumulated via a functional decoupling from climate during low climate variability in the late Holocene. Given the geologically short time span of our study (14 kyr), evolutionary forcing on TERs is not expected to override general trait–climate relationships (e.g., Davis et al., 2005). These differential responses observed between the two periods could be biased by numerical artefacts from a stronger magnitude of temperature forcing triggering higher response fit values (negative and positive) during the 14–7 ka period. Indeed, steeper environmental changes are expected to increase correlations numerically between the response variable and the environment. To accommodate for this bias towards higher response fit values observed during the high-variability period (and dealing with the resulting U-shaped distributions), we used one-sample Wilcoxon signed rank tests comparing the median of each period with zero. We based our interpretation of the results on the number of positive correlations rather than on the absolute strength of the correlation. Furthermore, the standard deviation of environmental time series did increase with the magnitude of environmental change (Supporting Information Text S2), reducing any neutral statistical artefacts that could, in theory, generate the reported correlation coefficients. A finer examination of our results also showed that changes in functional composition (for leaf area and LDMC) remained strong in the presence of small temperature and precipitation forcings (Supporting Information Figure S5), suggesting that variation in non-climatic factors might influence T-TERs. If the variables used in our study are able to represent correctly the climate forcing underlying changes in functional diversity during the study period, the functional disequilibrium might have arisen from

a trait–climate decoupling-driven non-climatic factors, rather than lagged responses driven by climate warming. Although we cannot totally rule out the possibility that temperature drives community dynamics, in part, in the late Holocene (because detecting a small effect of temperature statistically is challenging because of the low temperature variability), the hypothesis of non-climatic influence is consistent with a growing literature indicating that plant communities can undergo long-lasting compositional change driven by non-climatic factors. Such impacts might be relatively stronger when occurring against a backdrop of weak temperature change (Clifford & Booth, 2015). At a local scale, soil nutrient availability and land use have been shown to affect leaf trait community composition (Borgy, Violle, Choler, Denelle, et al., 2017; Ordoñez et al., 2009). Variations in fire regimens are also known to drive the global distribution of functional distribution, biomass and tree cover (e.g., Bond & Keeley, 2005; Bond et al., 2005). At large temporal scales, the late Pleistocene mammalian megafauna extinction in North America has also driven large changes in plant assemblages (Gill et al., 2009). These drivers are intrinsically linked and might ultimately be driven by human activities influencing trait distribution patterns via propagation, introduction and extinction of species (Abrams & Nowacki, 2008), fires (Bond & Keeley, 2005), erosion and land modifications (Borgy, Violle, Choler, Denelle, et al., 2017; Nowacki & Abrams, 2015). Moreover, our results are consistent with recent local-scale evidence showing that for some functional traits, community composition was more responsive to human disturbances than to climate change between 7 and 0 ka (Sande et al., 2019).

Alternatively, other potential explanations might underlie the apparent climate–trait decoupling observed during low climate variability. A first explanation lies in the choice of climate variables poorly describing how climate influences plant traits (Borgy, Violle, Choler, Denelle, et al., 2017; van Ommen Kloeke, Douma, Ordonez, Reich, & Van Bodegom, 2012). For example, bioclimatic factors, such as growing season length, might predict changes in functional traits better than integrative climate variables (such as temperature and precipitation; Borgy, Violle, Choler, Denelle, et al., 2017; van Ommen Kloeke et al., 2012). We ruled out this possibility by showing that growing season- and evapotranspiration-related bioclimatic variables were closely correlated with the maximum temperature in space and time and remained relatively stable during the late Holocene according to the climate modelling output used in the present study (Figure 2). However, abrupt changes in precipitation not captured by our climate model might have influenced plant community composition during the late Holocene. Simulations from CCSM3 model based on a 200-year window suggest a stable climatic period between 7 and 0 ka (Lorenz et al., 2016), but other studies (Shuman et al., 2009) suggest that the north-east USA might have undergone repeated severe drought events during the 7–0 ka period. These short-term, high-frequency events might not be captured well by the temporal resolution of our climatic model and might still affect vegetation dynamics and ecosystem properties (Seddon et al., 2016; Shuman et al., 2009). Plant functional dynamics in North America between 7 and 0 ka might be influenced, to

some extent, by a nonlinear response to inter-annual hydroclimatic variability. Finally, high levels of stochastic colonization and extinction of species (Drake, 1990; Law & Daniel Morton, 1993) could also influence the functional composition of plant communities. The imprint of such processes might be enhanced by the relatively weaker influence of deterministic processes during low climate variability.

Overall, our findings support the possibility of a non-climatic origin of current functional disequilibrium and call for a deeper investigation of the influence of non-climatic factors on large-scale community dynamics. Owing to the scarcity of data and the correlation between drivers, assessing the relative influence of human impact, land use, fire regimens or megafauna extinction on past biodiversity dynamics is challenging. Although local-scale studies can provide detailed information on climatic and non-climatic drivers at single sites over time (e.g., Sande et al., 2019), there is still insufficient knowledge to build reliable long-term datasets allowing for a formal test of their general effects on biodiversity dynamics. Another major challenge is that ecology has historically considered climate (and soils, to a lesser extent) as the only major and rapid driver of vegetation distribution (von Humboldt et al., 1805). Consequently, the impacts of other factors (e.g., human impacts) on functional biogeography have been overlooked, even though fossil records suggest that several non-climatic drivers have impacted past and current vegetation patterns (Pausas & Bond, 2019; Schrodt et al., 2019). Centennial-scale studies on the relative importance of climatic versus non-climatic drivers on plant community dynamics (Abrams & Nowacki, 2018; Nowacki & Abrams, 2015; Pederson et al., 2015) and long-term studies of contemporary vegetation changes (Danneyrolles et al., 2019) provided evidence for a strong influence of anthropogenic disturbance relative to climate change. We argue that embracing non-climatic factors as drivers of spatial and temporal associations between functional traits and the environment is a necessary step to gaining a better understanding and predicting future community dynamics.

4.1 | Concluding remarks

Our study shows that (a) temporal and spatial dynamics of functional composition can differ over continental spatial scales and millennial temporal scales, and (b) deviation from the equilibrium state is pervasive. However, (c) temporal trait dynamics observed during Holocene climate warming corresponded to expectations from spatial trait–climate associations, whereas (d) the functional composition of plant communities appears to decouple statistically from climate dynamics during periods of low climate variability. We argue that linking trait measurement data, palaeoecological records of assemblage composition (Birks et al., 2016) and climate dynamics (Lorenz et al., 2016) can provide valuable insights for functional biogeography over long temporal scales. Temporal perspectives on functional ecology provide new opportunities to investigate how past climatic responses have shaped present-day patterns of functional composition.

DATA AVAILABILITY STATEMENT

All analyses were carried out with R statistical software, v.3.4.4 (2018-03-15). The code used to perform the analyses and the functions used to compute the summary statistics can be found at: https://github.com/pgauzere/TER_CRD. TRY and TTT dataset can be accessed upon request at https://www.try-db.org/TryWeb/Home.php. The presence/absence matrices of pollen taxa at each site per time slice and a list of final sites are available at the Dryad data repository (http://dx.doi.org/10.5061/dryad.hk400). Community, climatic and CRD variables at each site per time slice per period per trait are available at: https://doi.org/10.5061/dryad.z612jm695

ORCID

Pierre Gaüzère [iD] https://orcid.org/0000-0003-1259-6131
Cyrille Violle [iD] https://orcid.org/0000-0002-2471-9226

REFERENCES

Abrams, M. D., & Nowacki, G. J. (2008). Native Americans as active and passive promoters of mast and fruit trees in the eastern USA. *Holocene*, *18*, 1123–1137.

Abrams, M. D., & Nowacki, G. J. (2018). Large-scale catastrophic disturbance regimes can mask climate change impacts on vegetation—A reply to Pederson et al. (2014) [Review of Large-scale catastrophic disturbance regimes can mask climate change impacts on vegetation—A reply to Pederson et al. (2014)]. *Global Change Biology*, *24*(1), e395–e396.

Bertrand, R., Riofrío-Dillon, G., Lenoir, J., Drapier, J., de Ruffray, P., Gégout, J.-C., & Loreau, M. (2016). Ecological constraints increase the climatic debt in forests. *Nature Communications*, *7*, 12643.

Birks, H. J. B., Felde, V. A., Bjune, A. E., Grytnes, J.-A., Seppä, H., & Giesecke, T. (2016). Does pollen-assemblage richness reflect floristic richness? A review of recent developments and future challenges. *Review of Palaeobotany and Palynology*, *228*, 1–25.

Birks, H. J. B., & Seppä, H. (2004). Pollen-based reconstructions of late-Quaternary climate in Europe—Progress, problems, and pitfalls. *Acta Palaeobotanica*, *44*, 317–334.

Bjorkman, A. D., Myers-Smith, I. H., Elmendorf, S. C., Normand, S., Rüger, N., Beck, P. S. A., … Weiher, E. (2018). Plant functional trait change across a warming tundra biome. *Nature*, *562*(7725), 57–62.

Bjorkman, A. D., Myers-Smith, I. H., Elmendorf, S. C., Normand, S., Thomas, H. J. D., Alatalo, J. M., …Baruah, G. (2018). Tundra Trait Team: A database of plant traits spanning the tundra biome. *Global Ecology and Biogeography*, *27*, 1402–1411.

Blois, J. L., Williams, J. W., Fitzpatrick, M. C., Ferrier, S., Veloz, S. D., He, F., … Otto-Bliesner, B. (2013). Modeling the climatic drivers of spatial patterns in vegetation composition since the Last Glacial Maximum. *Ecography*, *36*, 460–473.

Blois, J. L., Williams, J. W., Fitzpatrick, M. C., Jackson, S. T., & Ferrier, S. (2013). Space can substitute for time in predicting climate-change effects on biodiversity. *Proceedings of the National Academy of Sciences USA*, *110*, 9374–9379.

Blois, J. L., Williams, J. W. (Jack), Grimm, E. C., Jackson, S. T., & Graham, R. W. (2011). A methodological framework for assessing and reducing temporal uncertainty in paleovegetation mapping from late-Quaternary pollen records. *Quaternary Science Reviews*, *30*, 1926–1939. https://doi.org/10.1016/j.quascirev.2011.04.017

Blonder, B., Enquist, B. J., Graae, B. J., Kattge, J., Maitner, B. S., Morueta-Holme, N., … Violle, C. (2018). Late Quaternary climate legacies in contemporary plant functional composition. *Global Change Biology*, *24*, 4827–4840.

Blonder, B., Moulton, D. E., Blois, J., Enquist, B. J., Graae, B. J., Macias-Fauria, M., … Svenning, J. C. (2017). Predictability in community dynamics. *Ecology Letters*, *20*, 293–306.

Bond, W. J., & Keeley, J. E. (2005). Fire as a global "herbivore": The ecology and evolution of flammable ecosystems. *Trends in Ecology and Evolution*, *20*, 387–394.

Bond, W. J., Woodward, F. I., & Midgley, G. F. (2005). The global distribution of ecosystems in a world without fire. *The New Phytologist*, *155*, 525–538.

Borgy, B., Violle, C., Choler, P., Denelle, P., Munoz, F., Kattge, J., … Garnier, E. (2017). Plant community structure and nitrogen inputs modulate the climate signal on leaf traits. *Global Ecology and Biogeography*, *26*, 1138–1152.

Borgy, B., Violle, C., Choler, P., Garnier, E., Kattge, J., Loranger, J., … Viovy, N. (2017). Sensitivity of community-level trait–environment relationships to data representativeness: A test for functional biogeography. *Global Ecology and Biogeography*, *26*, 729–739.

Brewer, S., Jackson, S. T., & Williams, J. W. (2012). Paleoecoinformatics: Applying geohistorical data to ecological questions. *Trends in Ecology and Evolution*, *27*, 104–112.

Bruelheide, H., Dengler, J., Purschke, O., Lenoir, J., Jiménez-Alfaro, B., Hennekens, S. M., … Jandt, U. (2018). Global trait–environment relationships of plant communities. *Nature Ecology & Evolution*, *2*, 1906–1917.

Chave, J., Coomes, D., Jansen, S., Lewis, S. L., Swenson, N. G., & Zanne, A. E. (2009). Towards a worldwide wood economics spectrum. *Ecology Letters*, *12*, 351–366.

Clifford, M. J., & Booth, R. K. (2015). Late-Holocene drought and fire drove a widespread change in forest community composition in eastern North America. *Holocene*, *25*, 1102–1110.

Danneyrolles, V., Dupuis, S., Fortin, G., Leroyer, M., de Römer, A., Terrail, R., … Arseneault, D. (2019). Stronger influence of anthropogenic disturbance than climate change on century-scale compositional changes in northern forests. *Nature Communications*, *10*, 1265.

Davis, M. B. (1984). Climatic instability, time, lags, and community disequilibrium. In T. J. C. Jared Diamond (Ed.), *Community ecology* (269–296). New York: Harper and Row.

Davis, M. B., Shaw, R. G., & Etterson, J. R. (2005). Evolutionary responses to changing climate. *Ecology*, *86*, 1704–1714.

Drake, J. A. (1990). The mechanics of community assembly and succession. *Journal of Theoretical Biology*, *147*, 213–233. https://doi.org/10.1016/s0022-5193(05)80053-0

Enquist, B. J., Norberg, J., Bonser, S. P., Violle, C., Webb, C. T., Henderson, A., … Savage, V. M. (2015). Chapter nine—scaling from traits to ecosystems: Developing a general trait driver theory via integrating trait-based and metabolic scaling theories. In S. Pawar, G. Woodward, & A. I. Dell (Eds.), *Advances in ecological research* (Vol. *52*, pp. 249–318). Academic Press.

Garnier, E., Navas, M.-L., & Grigulis, K. (2016). *Plant functional diversity: Organism traits, community structure, and ecosystem properties*. Oxford: Oxford University Press.

Gaüzère, P., Iversen, L. L., Barnagaud, J.-Y., Svenning, J.-C., & Blonder, B. (2018). Empirical predictability of community responses to climate change. *Frontiers in Ecology and Evolution*, *6*(November), 186. https://doi.org/10.3389/fevo.2018.00186

Gill, J. L., Williams, J. W., Jackson, S. T., Lininger, K. B., & Robinson, G. S. (2009). Pleistocene megafaunal collapse, novel plant communities, and enhanced fire regimes in North America. *Science*, *326*(5956), 1100–1104.

Grime, J. P. (1974). Vegetation classification by reference to strategies. *Nature*, *250*(5461), 26–31.

Harrison, S. P., Bartlein, P. J., Brewer, S., Prentice, I. C., Boyd, M., Hessler, I., … Willis, K. (2014). Climate model benchmarking with glacial and mid-Holocene climates. *Climate Dynamics*, *43*, 671–688.

Karger, D. N., Conrad, O., Böhner, J., Kawohl, T., Kreft, H., Soria-Auza, R. W., … Kessler, M. (2017). Climatologies at high resolution for the earth's land surface areas. *Scientific Data*, *4*, 170122. https://doi.org/10.1038/sdata.2017.122

Kattge, J., Bönisch, G., Díaz, S., Lavorel, S., Prentice, I. C., Leadley, P., … Wirth, C. (2020). TRY plant trait database—Enhanced coverage and open access. *Global Change Biology*, *26*, 119–188.

Kattge, J., Díaz, S., Lavorel, S., Prentice, I. C., Leadley, P., Bönisch, G., … Wirth, C. (2011). TRY—A global database of plant traits. *Global Change Biology*, *17*, 2905–2935.

Keddy, P. A. (1992). Assembly and response rules: Two goals for predictive community ecology. *Journal of Vegetation Science*, *3*, 157–164. https://doi.org/10.2307/3235676

Keeley, J. E., Bond, W. J., Bradstock, R. A., Pausas, J. G., & Rundel, P. W. (2011). *Fire in Mediterranean ecosystems: Ecology, evolution and management*. Cambridge : Cambridge University Press.

Laughlin, D. C. (2014). Applying trait-based models to achieve functional targets for theory-driven ecological restoration. *Ecology Letters*, *17*, 771–784.

Lavorel, S., & Garnier, E. (2002). Predicting changes in community composition and ecosystem functioning from plant traits: Revisiting the Holy Grail. *Functional Ecology*, *16*, 545–556. https://doi.org/10.1046/j.1365-2435.2002.00664.x

Law, R., & Morton, R. D. (1993). Alternative permanent states of ecological communities. *Ecology*, *74*, 1347–1361. https://doi.org/10.2307/1940065

Liu, Z., Otto-Bliesner, B. L., He, F., Brady, E. C., Tomas, R., Clark, P. U., … Cheng, J. (2009). Transient simulation of last deglaciation with a new mechanism for Bølling-Allerød warming. *Science*, *325*(5938), 310–314.

Lorenz, D. J., Nieto-Lugilde, D., Blois, J. L., Fitzpatrick, M. C., & Williams, J. W. (2016). Downscaled and debiased climate simulations for North America from 21,000 years ago to 2100AD [Review of *Downscaled and debiased climate simulations for North America from 21,000 years ago to 2100AD*]. *Scientific Data*, *3*, 160048.

Maguire, K. C., Nieto-Lugilde, D., Blois, J. L., Fitzpatrick, M. C., Williams, J. W., Ferrier, S., & Lorenz, D. J. (2016). Controlled comparison of species- and community-level models across novel climates and communities. *Proceedings of the Royal Society B: Biological Sciences*, *283*(1826), 20152817. https://doi.org/10.1098/rspb.2015.2817.

Mathieu, J., & Davies, T. J. (2014). Glaciation as an historical filter of below-ground biodiversity. *Journal of Biogeography*, *41*, 1204–1214.

Moles, A. T., Perkins, S. E., Laffan, S. W., Flores-Moreno, H., Awasthy, M., Tindall, M. L., ... Bonser, S. P. (2014). Which is a better predictor of plant traits: Temperature or precipitation? *Journal of Vegetation Science*, *25*, 1167–1180.

Muscarella, R., & Uriarte, M. (2016). Do community-weighted mean functional traits reflect optimal strategies? *Proceedings of the Royal Society B: Biological Sciences*, *283*(1827), 20152434.

Nieto-Lugilde, D., Maguire, K. C., Blois, J. L., Williams, J. W., & Fitzpatrick, M. C. (2015). Close agreement between pollen-based and forest inventory-based models of vegetation turnover. *Global Ecology and Biogeography*, *24*, 905–916. https://doi.org/10.1111/geb.12300

Nowacki, G. J., & Abrams, M. D. (2015). Is climate an important driver of post-European vegetation change in the Eastern United States? *Global Change Biology*, *21*, 314–334.

Ordonez, A., & Svenning, J.-C. (2015). Geographic patterns in functional diversity deficits are linked to glacial-interglacial climate stability and accessibility. *Global Ecology and Biogeography*, *24*, 826–837.

Ordonez, A., & Svenning, J.-C. (2016). Functional diversity of North American broad-leaved trees is codetermined by past and current environmental factors. *Ecosphere*, *7*, e01237.

Ordonez, A., & Svenning, J.-C. (2017). Consistent role of Quaternary climate change in shaping current plant functional diversity patterns across European plant orders. *Scientific Reports*, *7*, 42988.

Ordoñez, J. C., Van Bodegom, P. M., Witte, J. P. M., Wright, I. J., Reich, P. B., & Aerts, R. (2009). A global study of relationships between leaf traits, climate and soil measures of nutrient fertility. *Global Ecology and Biogeography: A Journal of Macroecology*, *18*, 137–149.

Pausas, J. G., & Bond, W. J. (2019). Humboldt and the reinvention of nature. *The Journal of Ecology*, *107*, 1031–1037.

Pederson, N., D'Amato, A. W., Dyer, J. M., Foster, D. R., Goldblum, D., Hart, J. L., ... Williams, J. W. (2015). Climate remains an important driver of post-European vegetation change in the eastern United States. *Global Change Biology*, *21*, 2105–2110.

Pickett, S. T. A. (1989). Space-for-time substitution as alternative for long-term studies. In G. E. Likens (Ed.), *Long-term studies in ecology* (pp. 110–135). New York: Springer.

Pierce, S., Negreiros, D., Cerabolini, B. E. L., Kattge, J., Díaz, S., Kleyer, M., ... Tampucci, D. (2017). A global method for calculating plant CSR ecological strategies applied across biomes world-wide. *Functional Ecology*, *31*, 444–457.

Platt, J. R. (1964). Strong inference. *Science*, *146*(3642), 347–353.

Rohde, K. (2006). *Nonequilibrium ecology*. Cambridge: Cambridge University Press.

Sande, M. T., Gosling, W., Correa-Metrio, A., Prado-Junior, J., Poorter, L., Oliveira, R. S., ... Bush, M. B. (2019). A 7000-year history of changing plant trait composition in an Amazonian landscape; The role of humans and climate. *Ecology Letters*, *22*, 925–935.

Schrodt, F., Santos, M. J., Bailey, J. J., & Field, R. (2019). Challenges and opportunities for biogeography—What can we still learn from von Humboldt? *Journal of Biogeography*, *46*, 1631–1642.

Seddon, A. W. R., Macias-Fauria, M., Long, P. R., Benz, D., & Willis, K. J. (2016). Sensitivity of global terrestrial ecosystems to climate variability. *Nature*, *531*(7593), 229–232.

Shipley, B., De Bello, F., Cornelissen, J. H. C., Laliberté, E., Laughlin, D. C., & Reich, P. B. (2016). Reinforcing loose foundation stones in trait-based plant ecology. *Oecologia*, *180*, 923–931.

Shuman, B. N., Newby, P., & Donnelly, J. P. (2009). Abrupt climate change as an important agent of ecological change in the Northeast U.S. throughout the past 15,000 years. *Quaternary Science Reviews*, *28*, 1693–1709.

Šímová, I., Violle, C., Svenning, J.-C., Kattge, J., Engemann, K., Sandel, B., ... Enquist, B. J. (2018). Spatial patterns and climate relationships of major plant traits in the New World differ between woody and herbaceous species. *Journal of Biogeography*, *45*, 895–916.

Svenning, J.-C., Eiserhardt, W. L., Normand, S., Ordonez, A., & Sandel, B. (2015). The influence of paleoclimate on present-day patterns in biodiversity and ecosystems. *Annual Review of Ecology, Evolution, and Systematics*, *46*, 551–572. https://doi.org/10.1146/annurev-ecolsys-112414-054314

Svenning, J.-C., & Sandel, B. (2013). Disequilibrium vegetation dynamics under future climate change. *American Journal of Botany*, *100*, 1266–1286.

Tomasových, A., & Kidwell, S. M. (2010). The effects of temporal resolution on species turnover and on testing metacommunity models. *The American Naturalist*, *175*, 587–606.

van Ommen Kloeke, A. E. E., Douma, J. C., Ordonez, J. C., Reich, P. B., & Van Bodegom, P. M. (2012). Global quantification of contrasting leaf life span strategies for deciduous and evergreen species in response to environmental conditions. *Global Ecology and Biogeography*, *21*, 224–235.

Violle, C., Reich, P. B., Pacala, S. W., Enquist, B. J., & Kattge, J. (2014). The emergence and promise of functional biogeography. *Proceedings of the National Academy of Sciences USA*, *111*, 13690–13696.

von Humboldt, A., & Bonpland, A. (1805). *Essai sur la géographie des plantes: accompagné d'un tableau physique des régions équinoxiales, fondé sur des mesures exécutées, depuis le dixième degré de latitude boréale jusqu'au dixième degré de latitude australe, pendant les années 1799, 1800, 1801, 1802 et 1803 /par Al. de Humdboldt et A. Bonpland; rédigée par Al. de Humboldt*. Paris: Chez Levrault, Schoell et compagnie, libraires. https://doi.org/10.5962/bhl.title.9309

Webb, T. (1986). Is vegetation in equilibrium with climate? How to interpret late-Quaternary pollen data. *Vegetatio*, *67*, 75–91. https://doi.org/10.1007/bf00037359

Westoby, M., Falster, D. S., Moles, A. T., Vesk, P. A., & Wright, I. J. (2002). Plant Ecological Strategies: Some Leading Dimensions of Variation Between Species. *Annual Review of Ecology and Systematics*, *33*(1), 125–159. http://dx.doi.org/10.1146/annurev.ecolsys.33.010802.150452

Williams, J. W., Grimm, E. C., Blois, J. L., Charles, D. F., Davis, E. B., Goring, S. J., ... Takahara, H. (2018). The neotoma paleoecology database, a multiproxy, international, community-curated data resource. *Quaternary Research*, *89*, 156–177.

Williams, J. W., & Jackson, S. T. (2007). Novel climates, no-analog communities, and ecological surprises. *Frontiers in Ecology and the Environment*, *5*, 475–482.

Williams, J. W., Shuman, B. N., & Webb, T. III. (2001). Dissimilarity analyses of late-Quaternary vegetation and climate in eastern North America. *Ecology*, *82*, 3346–3362.

Willis, K. J., & MacDonald, G. M. (2011). Long-term ecological records and their relevance to climate change predictions for a warmer world. *Annual Review of Ecology, Evolution, and Systematics*, *42*, 267–287.

Woodward, F. I., & Williams, B. G. (1987). Climate and plant distribution at global and local scales. *Vegetatio*, *69*, 189–197.

Wright, I. J., Dong, N., Maire, V., Prentice, I. C., Westoby, M., Díaz, S., ... Reich, P. B. (2017). Global climatic drivers of leaf size. *Science*, *12*(6354), 917–921.

Wright, I. J., Reich, P. B., Cornelissen, J. H. C., Falster, D. S., Garnier, E., Hikosaka, K., ... Westoby, M. (2005). Assessing the generality of global leaf trait relationships. *The New Phytologist*, *166*, 485–496.

Wright, I. J., Reich, P. B., Westoby, M., Ackerly, D. D., Baruch, Z., Bongers, F., … Villar, R. (2004). The worldwide leaf economics spectrum. *Nature*, *428*(6985), 821–827.

SUPPORTING INFORMATION

Additional supporting information may be found online in the Supporting Information section.